

Actin Depolymerization in Dedifferentiated Liver Sinusoidal Endothelial Cells Promotes Fenestrae Re-Formation

Julie Di Martino,^{1,2*} Patrice Mascalchi,^{2,3*} Philippe Legros,⁴ Sabrina Lacomme,^{2,3} Etienne Gontier,^{2,3} Paulette Bioulac-Sage,¹ Charles Balabaud,¹ Violaine Moreau,^{1,2} and Frédéric Salte^{1,2}

Liver sinusoidal endothelial cells (LSECs) possess fenestrae, which are key for the exchange between blood and hepatocytes. Alterations in their number or diameter have important implications for hepatic function in liver diseases. They are lost early in the development of hepatic fibrosis through a process called capillarization. In this study, we aimed to demonstrate whether *in vitro* dedifferentiated LSECs that have lost fenestrae are able to re-form these structures. Using stimulated emission depletion super-resolution microscopy in combination with transmission electron microscopy, we analyzed fenestrae formation in a model mimicking the capillarization process *in vitro*. Actin is known to be involved in fenestrae regulation in differentiated LSECs. Using cytochalasin D, an actin-depolymerizing agent, we demonstrated that dedifferentiated LSECs remain capable of forming fenestrae. **Conclusion:** We provide a new insight into the complex role of actin in fenestrae formation and in the control of their size and show that LSEC fenestrae re-formation is possible, suggesting that this process could be used during fibrosis regression to try to restore exchanges and hepatocyte functions. (*Hepatology Communications* 2019;3:213-219).

The liver plays crucial roles for body homeostasis related to metabolism, immunity, and detoxification, to name a few. To fully handle these functions, the liver is highly vascularized. Indeed, the rich microvasculature ensures effective exchange with the circulating blood. Sinusoids devoid of basement membrane are present between each hepatocyte plate. Liver sinusoidal endothelial cells

(LSECs) that compose this endothelium present with specific features. They possess small transcellular pores called fenestrae,⁽¹⁾ which form a direct connection between the blood circulation and hepatocytes to improve exchange. Fenestrae are approximately 50 to 200 nm in diameter and are organized in sieve plates.⁽²⁾ In the past, they were studied using electron microscopy; however, they are increasingly being

Abbreviations: cyto D, cytochalasin D; LSEC, liver sinusoidal endothelial cell; PBS, phosphate-buffered saline; STED, stimulated emission depletion; TEM, transmission electron microscopy.

Received July 22, 2018; accepted November 14, 2018.

Additional Supporting Information may be found at onlinelibrary.wiley.com/doi/10.1002/hep4.1301/supinfo.

Supported by INSERM/Région Aquitaine (Ph.D. fellowship to J.D.M.), the Association Française pour la Recherche du Foie (AFEF), Agence Nationale de la Recherche (ANR-13-JJC-JSV1-0005), La Ligue Nationale Contre le Cancer, the Fondation ARC pour la Recherche sur le Cancer, Institut National du cancer (INCa PLBIO15-135 to F.S.), and the National Infrastructure France-BioImaging (ANR-10-INBS-04-0 to P.M.).

Present address for Julie Di Martino is TISCH Cancer Institute, Icahn School of Medicine at Mount Sinai Hospital, New York, NY.

*These authors contributed equally to this work.

© 2018 The Authors. *Hepatology Communications* published by Wiley Periodicals, Inc., on behalf of the American Association for the Study of Liver Diseases. This is an open access article under the terms of the Creative Commons Attribution-NonCommercial-NoDerivs License, which permits use and distribution in any medium, provided the original work is properly cited, the use is non-commercial and no modifications or adaptations are made.

View this article online at wileyonlinelibrary.com.

DOI 10.1002/hep4.1301

Potential conflict of interest: Nothing to report.

observed and analyzed using optical super-resolution or atomic force microscopy.⁽³⁻⁷⁾ Recently, we established a simple approach to visualize and analyze LSEC fenestrae⁽⁸⁾ using stimulated emission depletion (STED) microscopy.

LSECs are key cells in the hepatic fibrosis initiation process, regression of hepatic fibrosis, and liver regeneration.⁽⁹⁻¹¹⁾ At the beginning of the fibrosis process, capillarization occurs corresponding to the loss of fenestrae and the basement membrane surrounding the capillaries appears due to the accumulation of extracellular matrix deposition.⁽¹²⁾ To study fenestrae *in vitro*, we used primary LSECs isolated from mouse liver because no other cell type presents with these structures *in vitro*. In cell culture, LSECs dedifferentiate and lose their fenestrae, mimicking a capillarization-like process.⁽¹³⁾ Moreover, LSEC fenestrae diameter and number vary with drug treatments or environmental conditions, such as temperature, hypoxia, calcium flow, and pressure.⁽¹⁴⁾ Actin-targeting drugs, such as cytochalasin D (cyto D), latrunculin A, and jasplakinolide, have been reported to increase their number in differentiated cells while simultaneously decreasing the diameter of the fenestrae.⁽¹⁵⁻¹⁷⁾ Cyto D, an actin depolymerizing agent, is a cell-permeable fungal toxin that binds the barbed end of the actin filament, inhibiting the association and dissociation of G-actin subunits. The cytochalasin family is composed of eight members (A to J), and their efficiency to block actin filament elongation is variable. For example, some studies show that cyto D effects are progressive in cell culture compared to the transient impact of latrunculin B.⁽¹⁸⁾ Latrunculins are another family of toxins targeting actin; they are extracted from sponges and bind actin monomers, preventing actin polymerization. Several other actin toxins have been used on LSEC fenestrae.

In this study, we used cyto D to test the ability of dedifferentiated LSECs to re-form fenestrae.

Materials and Methods

LSEC ISOLATION AND CULTURE

LSECs were isolated from U.S. Naval Medical Research Institute male mice aged >15 weeks. Livers of two mice were excised for each experiment, perfused with Liberase DH (70 µg/mL final; Roche) and cut into pieces. A total of 40 mice were used for this work (20 experiments). After 20 minutes of digestion at 37°C, the lysate was ground in successive filters (100 µm, followed by 40 µm pores; BD Biosciences), rinsed 3 times in phosphate-buffered saline (PBS), and centrifuged at 300g for 10 minutes without breaks. The pellet was resuspended in Roswell Park Memorial Institute medium (GIBCO), deposited on a Percoll gradient (top stage: 22.5% Percoll, 2.5% PBS 10X, 0.025% HCl 0.1 M in PBS 1X; bottom stage: 45% Percoll, 5% PBS 10X, 0.05% HCl 0.1 M in PBS 1X), and centrifuged at 1,500g for 20 minutes without breaks. The cells were withdrawn from the gradient interface, and LSECs were purified by differential adhesion of Kupffer cells in a plastic dish. Cells freshly isolated were spread in complete endothelial basal medium (EBM-2; Lonza CC3156) supplemented with endothelial growth medium (EGM-2 SingleQuots; Lonza CC-4176) and 1% penicillin-streptomycin (Gibco) on cover slips precoated with filtered 2% fetal bovine serum in 1X PBS. LSECs were treated with cyto D (Sigma-Aldrich) at a concentration of 2 µM for 30 minutes. Dimethyl sulfoxide alone was used as the vehicle control.

ARTICLE INFORMATION:

From the ¹INSERM, UMR1053, Bariton-Bordeaux Research in Translational Oncology, Bordeaux, France; ²Université de Bordeaux, Bordeaux, France; ³Bordeaux Imaging Center, Bordeaux, France; ⁴Plateforme Aquitaine de Caractérisation des Matériaux, Pessac, France.

ADDRESS CORRESPONDENCE AND REPRINT REQUESTS TO:

Frédéric Saltel, Ph.D.
INSERM UMR 1053
Université de Bordeaux
146 Rue Léo Saignat

33076 Bordeaux cedex, France
E-mail: frederic.saltel@inserm.fr
Tel.: +33 (0)5 57 57 17 71

STAINING

After cell washing with PBS (37°C), LSECs were treated with CellMask Orange (Molecular Probes, Invitrogen) for 5 to 10 minutes according to the manufacturer's recommendations. After washing, LSECs were fixed using paraformaldehyde (Delta Microscopies) and stained using phalloidin Atto 647N as described.⁽¹⁹⁾ Tubulin staining was performed using an anti- α -tubulin antibody (mouse, B-5-1-2; Santa Cruz Biotechnology) and an anti-mouse secondary antibody (FluoProbes 488; Interchim).

MICROSCOPY

Confocal microscopy, transmission electron microscopy (TEM), and scanning electron microscopy (SEM) (see Supporting Experimental Procedures) were conducted at the Bordeaux Imaging Center, Bordeaux University, a core facility of the French network France-BioImaging.

STED Microscopy

Super-resolution imaging of fixed cells was carried out using STED microscopy with CellMask Orange and phalloidin-Atto 647N for actin staining (Thermo Fisher Scientific). The sample was imaged with an inverted Leica SP8 STED microscope equipped with an oil immersion objective (Plan Apo 100 \times NA 1.4), white light laser 2, and internal hybrid detectors. A 660-nm continuous wavelength laser (22 MW/cm², measured at the output of the objective) was used for the depletion of CellMask Orange, whereas Atto 647N was depleted with a 775-nm pulsed laser (19 MW/cm², 80 MHz frequency, approximately 600-picosecond pulse length). With these settings, lateral resolutions of 70 to 80 nm could be reached for both acquisition channels. Excitation laser lines were 560 nm and 647 nm, respectively. For image acquisition, we used the following parameters: 20 nm pixel size; 6 times average per line; 200 Hz scan speed.

IMAGE PROCESSING AND ANALYSIS

STED images acquired from fixed cells were denoised using PureDenoise plugin (Biomedical Imaging Group, École Polytechnique Fédérale de

Lausanne, Lausanne, Switzerland) in ImageJ software (U.S. National Institutes of Health, Bethesda, MD), followed by a Richardson–Lucy deconvolution provided by a DeconvolutionLab2 plugin (10 iterations; synthetic point spread function with pupil units of 10, all other parameters as default). Confocal images were processed with two passes of convolve plugin in ImageJ using a 3 \times 3 kernel (1 1 1, 1 10 1, 1 1 1). For visualization purposes only, we loaded images in ImageJ software and applied a gamma correction of 0.7 for confocal fixed-cell STED. For contour detection of fenestrae, STED raw images were denoised using Huygens Professional (Scientific Volume Imaging, the Netherlands) Classical Maximum Likelihood Estimation deconvolution algorithm with three iterations and a signal-to-noise ratio of 1:2. Quantification of fenestrae size was then performed using an ImageJ macro to semi-automatically retrieve individual contour and mean diameter. Briefly, a first threshold was manually set to discard large dark features from fenestrae detection, e.g., background region when one edge of the cell can be seen. Second, a local minimum plugin (Find Maxima, set with light background) was used to identify the center of each fenestra. From this selection, the contour was determined using the ImageJ active contour method plugin (Level Set). An automated loop incrementing sensitivity of this tool was used to define the optimal contour result comparing the inner/outer mean intensity ratio. Area measurement was transformed as the final average diameter, assuming a circular shape formula. All results were displayed as graphs created with GraphPad Prism (GraphPad Software, San Diego, CA), and statistical tests were generated using the same software.

Results

DE NOVO FENESTRAE FORMATION IN DEDIFFERENTIATED LSECs FOLLOWING ACTIN DEPOLYMERIZATION

LSECs freshly isolated from mouse liver presented fenestrae organized in sieve plates 1 day after isolation. As described,⁽¹³⁾ LSECs *in vitro* promptly dedifferentiated and lost their fenestrae. This loss was monitored using STED microscopy in cultured cells. Six days after isolation, we observed that cells dedifferentiated

without fenestrae in their membranes (Fig. 1A). This fenestrae loss is reminiscent of what occurs in the capillarization process during fibrotic disorder. Therefore, we used this model to test the reversibility of fenestrae loss. After 6 days of dedifferentiation in culture, LSECs were more spread out. Quantification of the cell area showed a 2-fold increase on day 6 after

isolation (Supporting Fig. S1). Actin has historically been known to regulate fenestrae number and size.⁽¹⁾ Hence, we decided to treat dedifferentiated LSECs with an actin-depolymerizing agent. Because cyto D treatment allows formation of new fenestrae in differentiated LSECs, we hypothesized that it could induce fenestrae re-formation in dedifferentiated LSECs

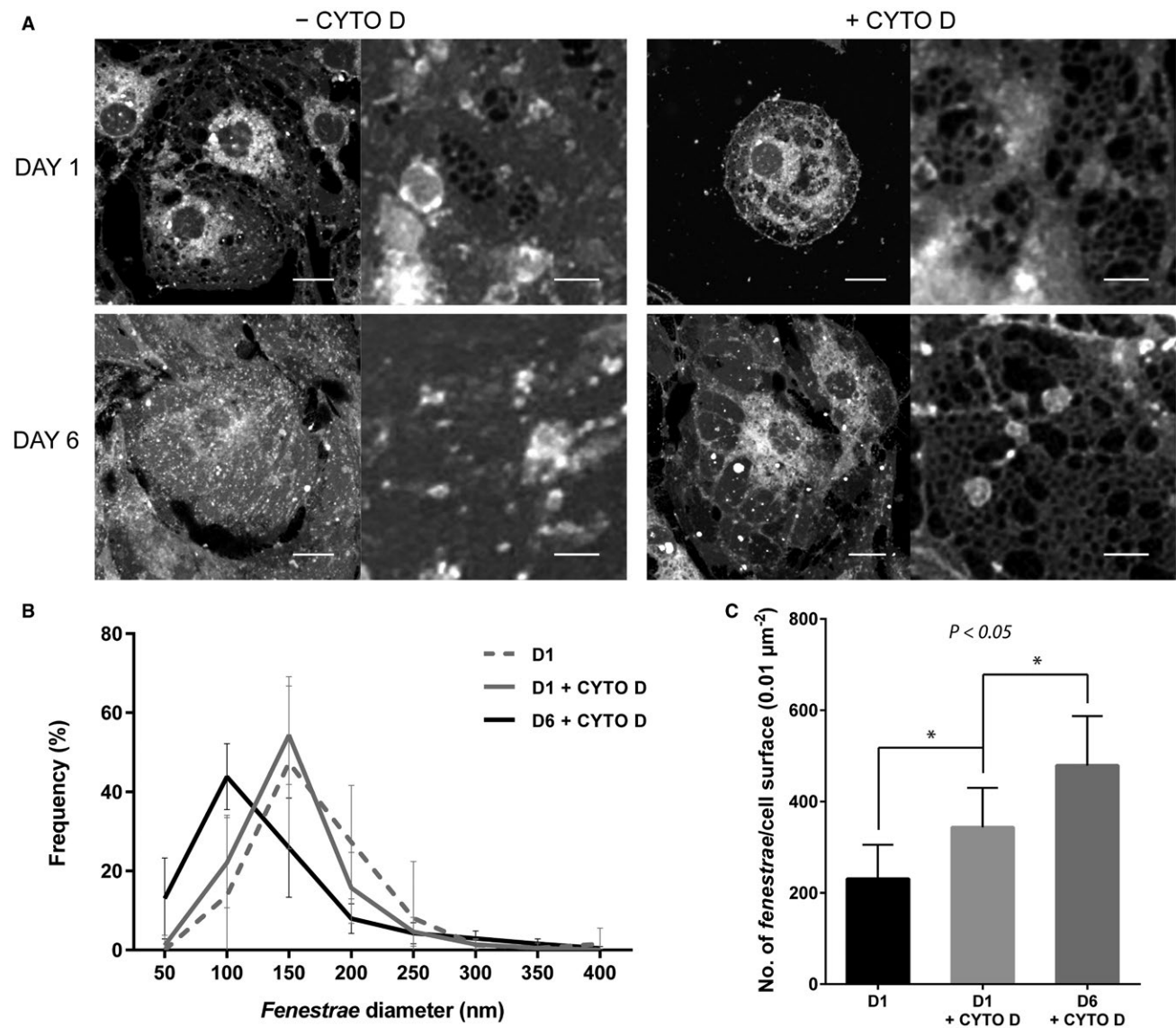


FIG. 1. Cyto D treatment allows fenestrae formation in dedifferentiated LSECs. (A) Confocal and STED images of LSEC on days 1 and 6 stained with CellMask and treated or not with cyto D. For each condition, we show a representative confocal image of cells at low magnification (left) and a STED image of fenestrae at high magnification (right). Scale bars represent $10 \mu\text{m}$ and $1 \mu\text{m}$, respectively. (B) Quantification of fenestrae size distribution with day 1/day 6 + cyto D or without cyto D treatment. Fenestrae were detected in a minimum of six different STED images captured from at least three different cells from three different experiments. The x axis values represent bin centers. Error bars correspond to SD. (C) Average number of fenestrae per unit of cell surface ($0.01 \mu\text{m}^2$). Statistical difference was evaluated using the unpaired Mann-Whitney t test with a 2-tailed P value; $*P < 0.05$. Error bars represent SD. Abbreviation: D, day.

devoid of fenestrae. Interestingly, we were able to re-create fenestrae in 6-day-long cultured dedifferentiated cells (Fig. 1A). We validated these data using SEM and TEM microscopy (Supporting Fig. S2).

Depending on the experiment, the percentage of cells that are able to re-create fenestrae varies from 40% to 70%. This is probably due to the cell isolation process and/or cell heterogeneity. Representative images of experiments performed more than 20 times using 40 livers are shown in Fig. 1. Using images obtained from STED microscopy, we quantified the size and number of fenestrae per unit of cell surface in different conditions (Fig. 1C). After cyto D treatment on day 1, we noticed an increase in the number of total fenestrae while cell area remained unchanged. On day 6, a majority of fenestrae had a diameter of <125 nm, whereas fenestrae on day 1 with or without cyto D treatment were slightly larger (diameter mainly between 125 and 175 nm). Surprisingly, *de novo*-formed fenestrae on day 6 were more numerous per unit of cell surface (Fig. 1C).

F-ACTIN ORGANIZATION DURING FENESTRAE INDUCTION FOLLOWING CYTO D TREATMENT

In parallel, we analyzed the cytoskeleton under the different conditions. We confirmed that the actin and tubulin cytoskeletons completely reorganize during the dedifferentiation process. We noticed a linearization of the microtubules associated with an increase of actin stress fibers along the LSEC culture (Supporting Fig. S3). At the cell scale, we noticed that cyto D treatment had reset the actin and tubulin organization observed in differentiated LSECs on day 1 (Supporting Fig. S3).

To fully understand the role of the actin cytoskeleton in this model, we combined two approaches, TEM and two-color STED microscopy. TEM revealed the presence of a clearly defined and dense cytoskeleton ring surrounding fenestrae on day 1 (Fig. 2A). Under cyto D treatment, F-actin is depolymerized, resulting in the destabilization of the majority of stress fibers (Fig. 2B). As described above, fenestrae appeared to be more numerous. In high-magnification TEM, we could still observe a less defined cytoskeleton ring surrounding each fenestrae (Fig. 2B). In this condition, STED microscopy showed a

maintenance and clear distribution of actin staining surrounding fenestrae. On day 6 in untreated cells, fenestrae disappeared and numerous actin stress fibers were observed using confocal, STED, or TEM techniques (Fig. 2C). Following cyto D treatment, *de novo*-formed fenestrae appeared without a surrounding cytoskeleton ring (Fig. 2D). It is important to note that even though there is no ring in TEM pictures, phalloidin staining is still present in re-formed fenestrae. As described earlier (Fig. 1B), fenestrae were smaller and more numerous compared to day 1 fenestrae. All these observations suggest that even if actin is not required for fenestrae formation, the presence of a complete cytoskeleton ring may control the diameter of fenestrae.

Discussion

LSEC fenestrae are important structures for liver physiology, and their loss is involved in several liver pathologies.⁽¹²⁾ Recently, we demonstrated that STED microscopy was suitable for LSEC fenestrae observation.⁽⁸⁾ Using this methodology in combination with TEM and an *in vitro* LSEC dedifferentiation model that mimics capillarization observed *in vivo*, we tested actin cytoskeleton involvement in fenestrae formation. We revealed that the cytoskeleton is closely associated with fenestrae and is organized in a dense ring surrounding them. Cyto D short-term treatment mainly removes large stress fibers, which were formed during LSEC dedifferentiation, and allows fenestrae re-formation. On day 6 after isolation, new fenestrae appeared with a smaller diameter following cyto D treatment. Interestingly, we noticed that LSECs are resistant to cyto D treatment compared to other endothelial cells. Indeed, human umbilical vein endothelial cells treated under the same conditions exhibit complete cell retraction (data not shown). TEM reveals the absence of a cytoskeleton ring around these new fenestrae. However, it is important to note that even if no ring is present in TEM pictures, phalloidin staining is still present in re-formed fenestrae. These observations support the idea that actin is a component of the cytoskeleton ring and drives the regulation of fenestrae diameter. After cyto D treatment at day 6 and in consequence to the absence of the cytoskeleton ring, the fenestrae average diameter was lower, so a higher number of fenestrae could be formed in the same area.

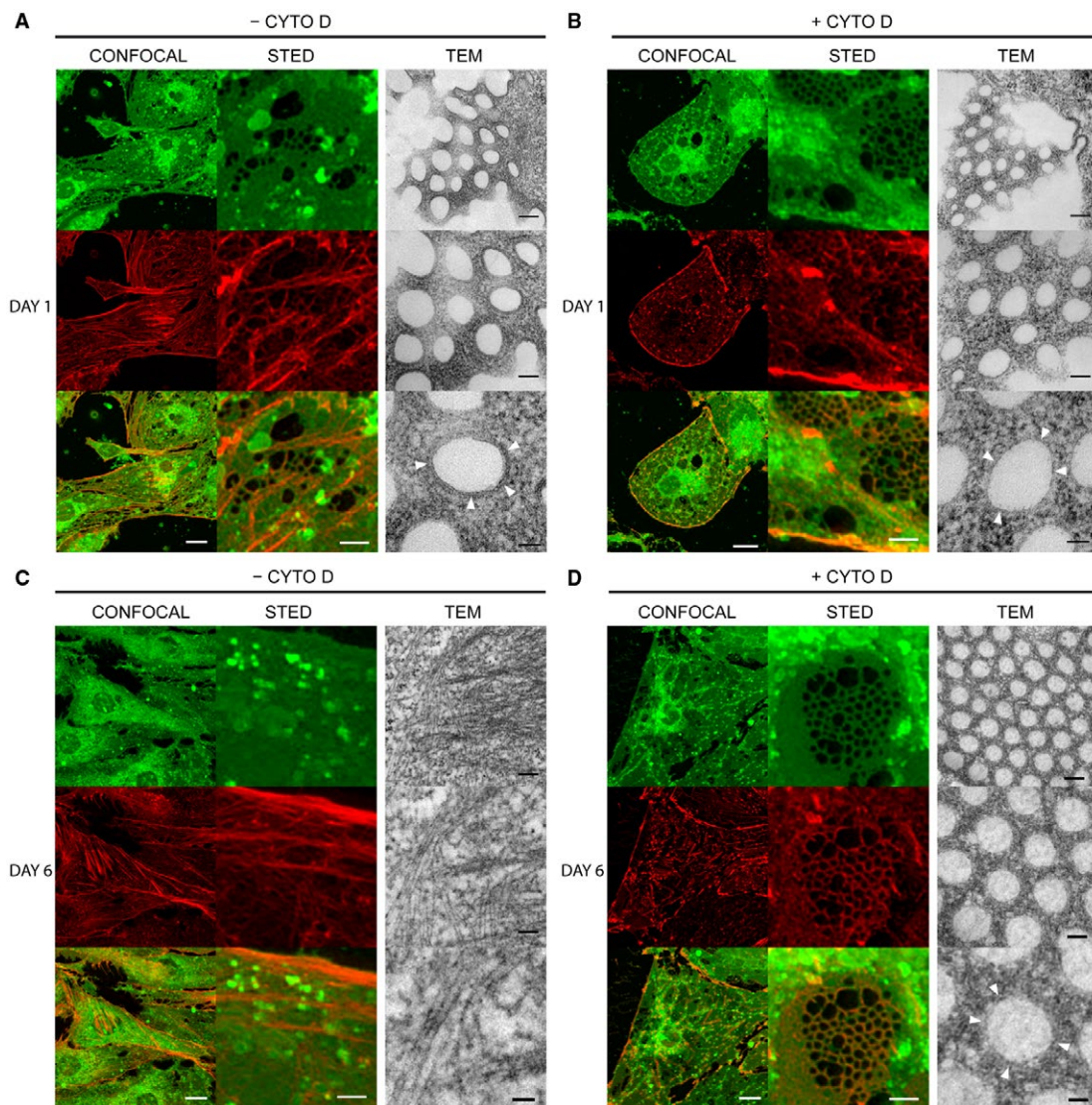


FIG. 2. Actin distribution in LSECs following cyto D treatment. (A–D) Representative confocal (low magnification, left columns) and STED (high magnification, middle columns) images of fenestrae (green, CellMask) and F-actin (red). The lower panel shows overlay of both stainings. The right column corresponds to increasing magnification views of a representative TEM image. Scale bars represent 10 μm and 1 μm , respectively, for confocal and STED images. Scale bars represent 200 nm, 100 nm, and 50 nm from upper to lower TEM images, respectively. (A) Untreated differentiated LSECs after 1 day of culture. Arrowheads point to dense ring-like element surrounding fenestrae in TEM image. (B) LSECs (day 1) after cyto D treatment, illustrating stress fiber loss. Arrowheads in TEM image indicate a low-density ring surrounding fenestrae. (C) Untreated dedifferentiated LSECs (day 6 of culture). TEM images illustrate presence of long fibers but not ring-like shapes. (D) Images of dedifferentiated LSECs (day 6) after cyto D treatment, illustrating stress fiber loss. Arrowheads in lower right TEM image point to a low-density and irregular layer surrounding fenestrae.

Our data suggest the coexistence of at least two different actin networks, one very sensitive to cyto D that forms stress fibers and a second one more resistant to the drug, possibly due to the formation of a complex network with other proteins that support fenestrae. Actin stress fibers seem to be incompatible with fenestrae formation. These structures could prevent contact

between upper and lower cell membranes and thus prevent their fusion. These observations emphasize the importance of identifying the exact composition of the cytoskeleton ring and molecules involved in membrane fusion. Identification of such a mechanism will also help us to understand how to control fenestrae opening and to design drugs that could slow down the

fibrosis progression or promote fibrosis reversion.⁽²⁰⁾ Indeed, after chronic injury, such as viral hepatitis or alcoholic disorder and nonalcoholic steatohepatitis, the liver develops fibrosis. Fibrosis is a slow process promoting an extracellular matrix accumulation, resulting in a general increase in organ stiffness.⁽²¹⁾ The progression of the disease leads to cirrhosis and ultimately to hepatocellular carcinoma.⁽²²⁾ Fenestrae loss is an early event in this pathology, and control of the fenestrae aperture could be an important element to help reverse the fibrosis process.

Acknowledgment: We thank Pierre Costet and technicians from the “animalerie conventionnelle” who helped take care of the animals. We also thank the Bordeaux Imaging Center, part of the national infrastructure of France-BioImaging, for access to confocal and STED super-resolution microscopes.

REFERENCES

- 1) Braet F, Wisse E. Structural and functional aspects of liver sinusoidal endothelial cell fenestrae: A review. *Comp Hepatol* 2002;1:1.
- 2) Wisse E. An electron microscopic study of the fenestrated endothelial lining of rat liver sinusoids. *J Ultrastruct Res* 1970;31:125-150.
- 3) Zapotoczny B, Szafranska K, Kus E, Braet F, Wisse E, Chlopicki S, et al. Tracking fenestrae dynamics in live murine liver sinusoidal endothelial cells. *Hepatology* 2018; doi:https://doi.org/10.1002/hep.30232.
- 4) **Monkemoller V, Oie C**, Hubner W, Huser T, McCourt P. Multimodal super-resolution optical microscopy visualizes the close connection between membrane and the cytoskeleton in liver sinusoidal endothelial cell fenestrations. *Sci Rep* 2015;5:16279.
- 5) Zapotoczny B, Szafranska K, Owczarczyk K, Kus E, Chlopicki S, Szymonski M. Atomic force microscopy reveals the dynamic morphology of fenestrations in live liver sinusoidal endothelial cells. *Sci Rep* 2017;7:7994.
- 6) Braet F, Wisse E. Gentle palpating liver sinusoidal endothelial cells reveals the dynamic behavior and formation of fenestrae: A new window for biomedical research. *Hepatology* 2018;67:2460-2461.
- 7) Braet F, Taatjes DJ, Wisse E. Probing the unseen structure and function of liver cells through atomic force microscopy. *Semin Cell Dev Biol* 2018;73:13-30.
- 8) Di Martino J, Mascalchi P, Legros P, Lacomme S, Gontier E, Bioulac-Sage P, et al. STED microscopy: A simplified method for liver sinusoidal endothelial fenestrae analysis. *Biol Cell* 2018;110:159-168.

- 9) **Xu M, Wang X**, Zou Y, Zhong Y. Key role of liver sinusoidal endothelial cells in liver fibrosis. *Biosci Trends* 2017;11:163-168.
- 10) DeLeve LD. Liver sinusoidal endothelial cells and liver regeneration. *J Clin Invest* 2013;123:1861-1866.
- 11) DeLeve LD. Liver sinusoidal endothelial cells in hepatic fibrosis. *Hepatology* 2015;61:1740-1746. Erratum in: *Hepatology* 2015;62:326.
- 12) **Poisson J, Lemoine S**, Boulanger C, Durand F, Moreau R, Valla D, et al. Liver sinusoidal endothelial cells: physiology and role in liver diseases. *J Hepatol* 2017;66:212-227.
- 13) Juin A, Planus E, Guillemot F, Horakova P, Albiges-Rizo C, Genot E, et al. Extracellular matrix rigidity controls podosome induction in microvascular endothelial cells. *Biol Cell* 2013;105:46-57.
- 14) Gatmaitan Z, Varticovski L, Ling L, Mikkelsen R, Steffan AM, Arias IM. Studies on fenestral contraction in rat liver endothelial cells in culture. *Am J Pathol* 1996;148:2027-2041.
- 15) Braet F, De Zanger R, Jans D, Spector I, Wisse E. Microfilament-disrupting agent latrunculin A induces and increased number of fenestrae in rat liver sinusoidal endothelial cells: comparison with cytochalasin B. *Hepatology* 1996;24:627-635.
- 16) Braet F, De Zanger R, Baekeland M, Crabbe E, Van Der Smissen P, Wisse E. Structure and dynamics of the fenestrae-associated cytoskeleton of rat liver sinusoidal endothelial cells. *Hepatology* 1995;21:180-189.
- 17) Spector I, Braet F, Shochet NR, Bubb MR. New anti-actin drugs in the study of the organization and function of the actin cytoskeleton. *Microsc Res Tech* 1999;47:18-37.
- 18) Spector I, Shochet NR, Blasberger D, Kashman Y. Latrunculins—novel marine macrolides that disrupt microfilament organization and affect cell growth: I. Comparison with cytochalasin D. *Cell Motil Cytoskeleton* 1989;13:127-144.
- 19) **Bar J, Kobler O**, van Bommel B, Mikhaylova M. Periodic F-actin structures shape the neck of dendritic spines. *Sci Rep* 2016;6:37136.
- 20) **Kong LJ, Li H**, Du YJ, Pei FH, Hu Y, Zhao LL, et al. Vatalanib, a tyrosine kinase inhibitor, decreases hepatic fibrosis and sinusoidal capillarization in CCl4-induced fibrotic mice. *Mol Med Rep* 2017;15:2604-2610.
- 21) Bataller R, Brenner DA. Liver fibrosis. *J Clin Invest* 2005;115:209-218.
- 22) Zhang DY, Friedman SL. Fibrosis-dependent mechanisms of hepatocarcinogenesis. *Hepatology* 2012;56:769-775.

Author names in bold designate shared co-first authorship.

Supporting Information

Additional Supporting Information may be found at onlinelibrary.wiley.com/doi/10.1002/hep4.1301/supinfo.